Journal of Hydrology: Regional Studies 30 (2020) 100701

Contents lists available at ScienceDirect

Journal of Hydrology: Regional Studies

journal homepage: www.elsevier.com/locate/ejrh

The hydrogeological situation after salt-mine collapses at Solotvyno, Ukraine

Leonard Stoeckl[a,*], Vanessa Banks[b], Stella Shekhunova[c], Yevgeniy Yakovlev[c]

[a] Federal Institute for Geosciences and Natural Resources (BGR), Stilleweg 2, 30655, Hannover, Germany
[b] British Geological Survey, Environmental Science Centre, Nicker Hill, Keyworth, United Kingdom
[c] National Academy of Sciences of Ukraine (NASU), Institute of Geological Sciences, Kyiv, Ukraine

ARTICLE INFO

Keywords:
Salt mine collapse
Contamination
Sinkhole formation
variable density flow
Tisza River

ABSTRACT

Study region: The study site is located in the south-western part of the Ukraine, in the area of the historical rock-salt mining town Solotvyno. The former mining area is situated in close vicinity to the River Tisza, the main tributary of the Danube River, the largest river in Europe.
Study focus: After uncontrolled flooding of several salt mines, a one month advisory mission was launched by the European Commission to estimate the impact of the abandoned salt mines (containing large quantities of salt water) on the environment. As a consequence of the flooding, dozens of sinkholes formed and sinkhole forming processes are ongoing, with sinkhole diameters reaching 250 m. As river contamination by the release of large quantities of saltwater would lead to an international disaster, hydrogeological measurements were taken on-site to study the system.
New hydrological insights of the region: At the study site, saturated (hyper-saline) water as well as fresh surface and groundwater were encountered in close vicinity to each other. Electrical conductivity, as a proxy for salinity, and temperature were measured on-site and water samples taken from surface-, ground- and mine waters were analyzed for chemistry and stable isotopes, providing new insights into groundwater flow dynamics. A conceptual model shows the salt dome, and potential flow paths from the mining area to the Tisza River, in the context of the mines and associated sinkholes potentially impacting the river water quality.

1. Introduction

Solotvyno is a historical rock-salt mining town, situated above a salt dome structure in the south west of Ukraine, close to its border with Romania. A legacy of the salt mining, there are at least nine abandoned salt mines of which the last two to operate were unexpectedly unintentionally flooded in 2010. Flooding occurred due to mine collapse triggered by underground mining operations. As a consequence, huge surface collapses developed, similar to the sinkholes in Berezniki, Russia, after flooding of the potash mining area in 2006 (Ashrafianfar et al., 2011).

An official request was presented to the European Commission by the Hungarian authorities, as a consequence of elevated salt concentrations in the Tisza River in 2008 (OLHGC, 2009). The Tisza River is the largest tributary of the Danube, which itself is the largest European river and of major ecological as well as economic importance for the several countries that border it. Sourced in the Carpathian Mountains, around 400 km upstream of the Solotvyno mining area, the Tisza River enters Hungary at Tiszabecs, around 104 km downstream. Here, chloride concentrations of 504 mg/l were measured in 2008. This concentration exceeds the proposed

* Corresponding author.
E-mail address: leonard.stoeckl@bgr.de (L. Stoeckl).

https://doi.org/10.1016/j.ejrh.2020.100701
Received 4 November 2019; Received in revised form 28 May 2020; Accepted 3 June 2020
Available online 25 June 2020

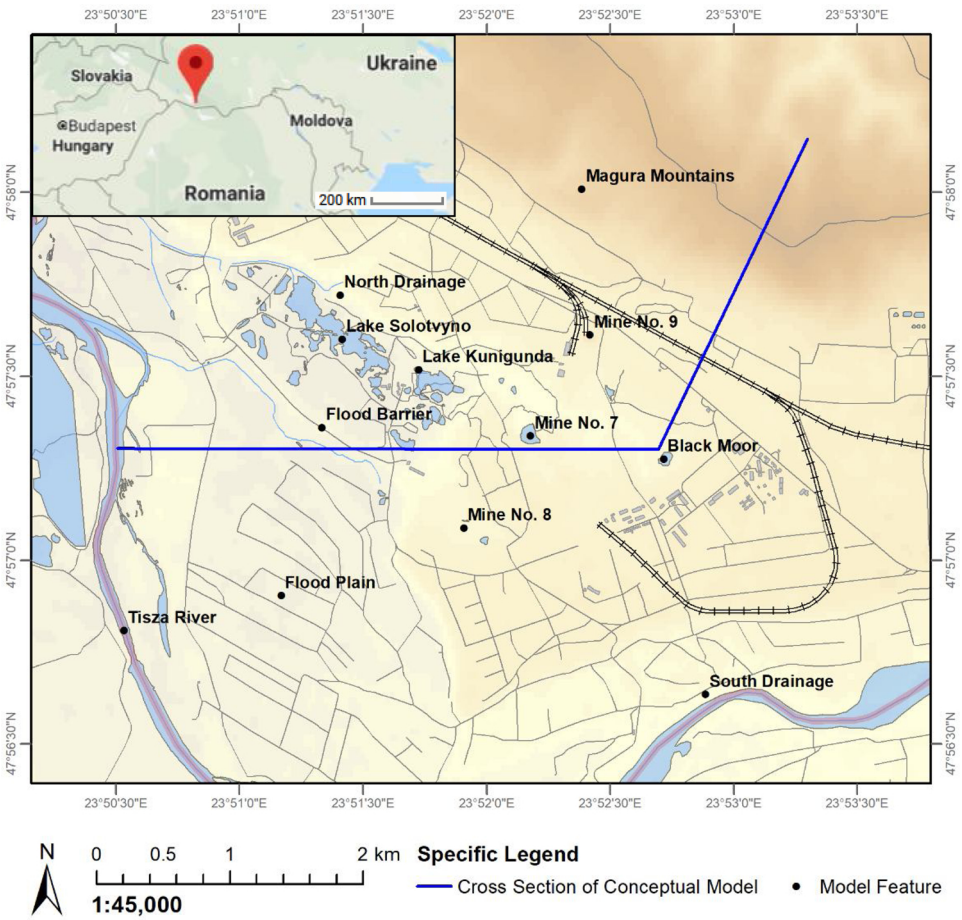

Fig. 1. Study area at the border of Romania and Ukraine (small overview map, google earth©) and Solotvyno with features of interest. The blue line indicates the location of the cross-section used in the conceptual model from the Tisza River to the Magura Mountains (Fig. 3).

surface water quality standard (SWQS) of 200 mg/l (OECD, 2008), thus alarming the Hungarian authorities.

The hydrogeological situation and the impact of anthropogenic mining activities on the area was not previously well understood. Velasco et al. (2017) performed ground deformation mapping and monitoring at Solotvyno using InSAR technology. The InSAR results served as an input for delimitating subsidence and landslide risk areas. The hydrogeology and the potential impact of large quantities of saline waters from the mines on the Tisza River, however, were not investigated. Onencan et al. (2018) have developed a participatory GIS risk mapping and citizen science approach for Solotvyno salt mines. Their aim is the creation of an online joint decision-making tool and map named iSOLOVTYNO by 2020.

This study gives an overview of the hydrogeological situation and the potential impacts of the Solotvyno mining area on the Tisza River. It is the result of a responsive field survey undertaken by the EUCPT (European Civil Protection Team) in collaboration with experts from the Institute of Geological Sciences, National Academy of Sciences of Ukraine (NASU). These results may serve as a hydrogeological baseline study and feed into the previously mentioned online decision-making tool.

1.1. Study area

The town of Solotvyno (47°57´0´´E; 23°52´0´´N) is situated between the Tisza River and the Magura Mountains at an elevation of around 280 m above sea level. The Tisza River meanders around the Solotvyno salt dome structure, forming the border between Ukraine to the north and Romania to the south.

The Magura Mountains stretch from north west to south east and are located south of the River Apshytsya. This mountain chain acts as a natural barrier and recharge area with altitudes of up to 400 m (Fig. 1). Average monthly precipitation is lowest in March (42 mm) and highest in June (101 mm) with an average annual recharge of around 744 mm/a. The average temperature is lowest in January (−3.5 °C) and highest in July (18.8 °C) with an annual average temperature of 8.8 °C (URL-I, 2020). The town is supplied with fresh water from a pumping station, which is located close to the most southern stretch of the river, at the border with Romania. The meander of the river at this location, is attributed to the uplift of the salt dome, which led to a successive southward displacement of the Tisza River in recent geological times. The general surface and near-surface runoff into the Tisza River has changed significantly over the last hundred years, influenced by the temporary drainage of mines, and other mining works as shafts and pits (Shekhunova et al., 2015).

The largest lake in the area, Solotvyno Lake (sometimes referred to as" Lake 18" and mistakenly shown as "Lake Kunigunda" in several sources, including google earth©), is located north west of the Solotvyno mining area. The top of the salt dome comes close to the surface, i.e. only metres below ground surface at a number of locations, with an outcrop exposed at Lake Kunigunda (see fresh & saltwater lakes in Fig. 1), a saturated saltwater lake. Streams, swamps and lakes influence karstification and erosion processes in the area. The smaller lakes, e.g. Lake Kunigunda, and ponds, which generally show higher salinity values, are situated south-east of Solotvyno Lake. These lakes are assumed to be the remnants of the historic sub-surface Mines No 1 to No 6. After abandonment, the mine chambers collapsed and formed these lakes. Today, Lake Kunigunda serves as a recreational area and was sampled during the mission. Anthropogenic modification of the area includes hand excavation of rock salt and redistribution of water from one "sub"-lake (divided by small dams) into another lake, presumably to maintain a specific water level for the tourists visiting this area. The lakes are situated in the zone between the top of the salt dome and the adjacent bedrock.

Contextually, the salt mines are situated within the Transcarpathian trough, a north-west to south-east trending linear feature 150 km in length and 20 to 35 km in width, formed by the collision zone of the Eurasian and Pannonian plates. It is a Neogene depression underlain by the heterogeneous Paleozoic and Mesozoic-Paleogene bases. The depth of the foundation varies from 670 to 1400 m (district of Uzhgorod) to around 2350 m below ground (district of Solotvyno; Glushko, 1968). The trough is confined to the zone of deep faults of the Carpathian extension that has been active for the last 3 million years. It is filled with Miocene-Holocene molasses, represented by clay and sandy-clay rocks, which include tufogenic and evaporates (i.e. rock-salt) strata. The evaporites formed within restricted basins associated with a Paratethys seaway that formed during the Badenian, around 14 Ma ago (Bukowski et al., 2007). The Transcarpathian trough has formed in a zone where the continental crust is reduced to thicknesses of between 25 and 27 km and is characterized by significant horizontal and vertical heterogeneity and stratification (Starostenko et al., 2013); a high heat flux up to 135 mW/m^2 (Gordienko et al., 2012; Kutas, 2014); active modern movements (Starostenko, 2015), and seismicity. It is crossed by both longitudinal and transverse fault systems. The geological setting at Solotvyno is displayed in Fig. 2, showing the proximity between the salt dome and the Tisza River. On the northern river bank Quaternary alluvial sediments have been laid down by the Tisza River during its progressive shift to the south.

In total, nine different mines were operated in Solotvyno, of which Mines No 1 to Mine No 6 were older and of a smaller operational scale, being operational until the 1930´s, latest. Mine No 7 was active until 1970. Its remains are located to the east of the Solotvyno lake area, i.e. towards the centre of the salt dome. Mine No 8 and Mine No 9 are located on the southern and northern flanks of the dome, respectively (Fig. 1), and were both abandoned after flooding in 2010.

Mine chambers in Mine No 7 and Mine No 8 collapsed, because they were excavated close to the surface with only 10 m–30 m of Quaternary sediments above the uppermost chambers (visible today at the flanks of the mine collapses). A layer of a clay and salt mixture (Pallag, Daupley et al., 2018), several decimeters in thickness, had formed as a capping on top of the rock salt. It is dissolution residue mixed with clay particles, which are transported towards the salt dome by the natural shallow groundwater flow. As a result of the reduced roof protection from above and in areas where the Pallag is absent, shallow groundwater could enter the mines after roof collapse, resulting in huge surface features, i.e. mine craters with diameters of around 250 m. Although Mine No 7 had already collapsed in 1950, it continued to be worked from Mine No 8 via a horizontal tunnel until it finally had to be abandoned in 1970.

Mine No 9 is situated in the northern part of the mining area and was worked to a greater depth of around 400 m below ground. No collapses are visible at the surface that could be directly linked to the flooding of Mine No 9. It is reported, however, that flooding of this mine occurred from the side, as it was excavated too close to the adjacent bedrock. Once water-bearing faults or discontinuities were struck, water flow into the mine chamber could not be stopped leading to rapid salt dissolution. Mine No 8, as well as Mine No 9, operated until around 2010, when flooding occurred.

In addition to the major collapses above the former mining area, smaller sinkholes formed in a number of different areas above the salt dome. These were predominantly in the area between Mine No 7, Mine No 8, and the Black Moor, which is a lake (or crater) feature, located at the upstream part of the study area, i.e. at the eastern margin of the salt dome (Fig. 1).

Fig. 3 shows a conceptual model of the cross-section from the Magura Mountains (upstream) via the salt dome area (central) to the Tisza River (downstream), following the blue line in Fig. 1. Sizes and objects are indicative and not to scale in this cross-section. The regional hydraulic gradient is broadly from east to west, following the natural gradient and flow direction of the Tisza River. Elevation drops steeply over the short stretch, of around 2 km, from the Magura Mountain ridge (up to 400 m a.s.l.) to the salt dome area in central Solotvyno (257 m to 295 m a.s.l.). A moderate surface gradient of about 30 m exists between the Tisza River at about 252 m a.s.l. and the central Solotvyno mining area at about 282 m a.s.l. over a distance of around 3 km. In the downstream area, several flow components are indicated. These are potential linkages between salt water and the River Tisza as well as flow from the ancient mine drainage systems, upwelling of deep groundwater, and enhanced flow in cracks, faults, or discontinuities in the bedrock. The conceptual model is also informed by the understanding that the formation of saline water requires several years to decades to reach saturation. This requires relatively long contact times of fresh water with the salt dome. Compared to fresh water, brines are characterized by high densities, e.g. 1.164 g/cm^3 or 22 % NaCl salt by weight, at ambient temperatures (Lide, 2004). This means that less dense fresh water is generally flowing above the rather immobile denser saltwater in greater depths. This has allowed us to systematically consider the potential impacts of prevailing salt water on fresh ground and surface waters in the former Solotvyno mining area.

Maintenance of the stability of the mine workings is a primary objective aimed at securing ground stability for the inhabitants of Solotvyno and minimizing the potential environmental impact on the Tisza River. This requires that they are protected from inputs of fresh water. Fresh water, which may lead to salt dissolution, can have several origins. The specific sources identified by this study are: 1) precipitation in the Solotvyno Mining area, 2) shallow subsurface water flow from the Magura Mountains, 3) hyporheic flow (i.e. Tisza River water which enters the Alluvium at one point in time/space, and returns to the Tisza River at another point in time/space), and 4) anthropogenic inputs such as leaking water services and agricultural irrigation. Another potential source of dissolution is the introduction of deep groundwater flow from the Magura or Carpathian Mountains. For these water sources to impact on the

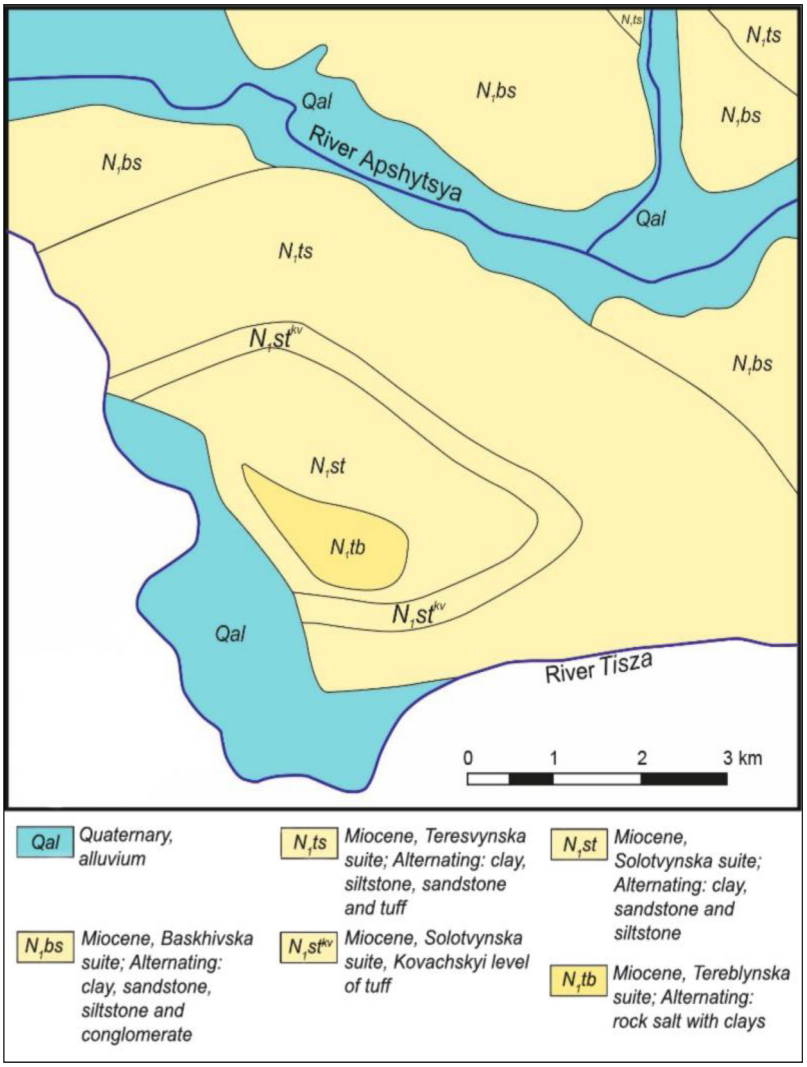

Fig. 2. Geological map of Solotvyno (modified from Frolov (1973).

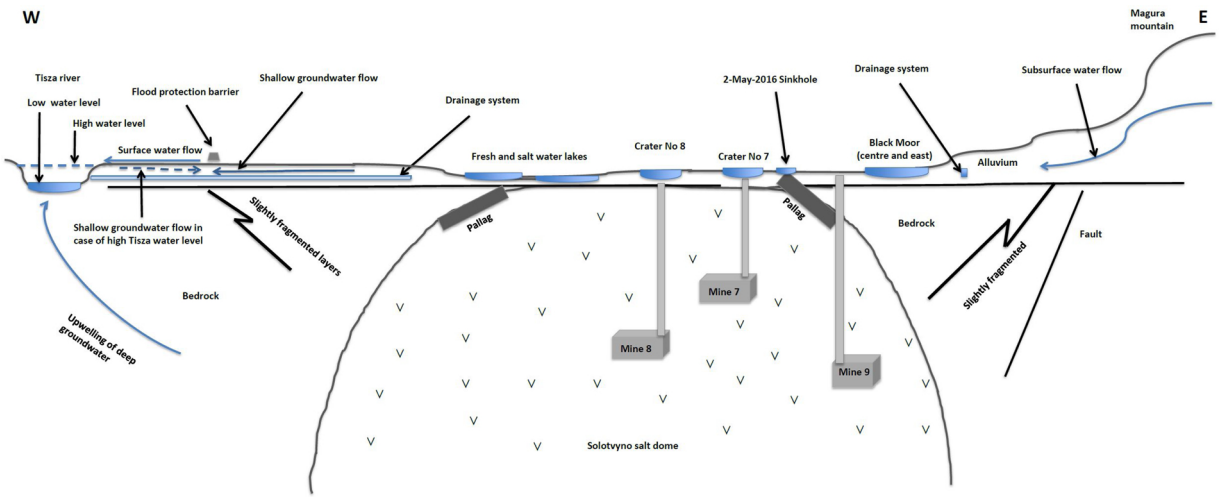

Fig. 3. Conceptual model indicating the relevant flow processes in the former mining area of Solotvyno and surroundings.

Solotvyno mine area, so called “hydrological windows” have to be present in order to allow a contact with the salt dome.

1.2. Methodology

A hydrogeological survey of the Solotvyno mining area, including the Tisza River and the Magura Mountains, was conducted by the EUCPT. All potential sampling locations in the study area were visited, e.g. different groundwater wells, mine shafts and craters, sinkholes, lakes and rivers. Nevertheless, some locations had to be neglected for sampling due to safety reasons, e.g. different abandoned mine shafts. For example, whilst the Black Moor and crater of Mine No 7 were entered by boat, the steep and unstable walls of the Mine No 8 crater precluded sampling.

In-situ water quality parameters (i.e. temperature, electrical conductivity (EC) and pH) were directly measured in the field whenever possible using either a handheld Hanna Instruments multi-probe or a WTW LF 196 conductivity meter attached to a 50 m cable. EC measurements were automatically corrected by the device for a standard temperature of 25 °C. The conductivity meter was also used to measure the water depth of lakes and craters at various locations by manually determining the point of resistance, i.e. when the probe touched the ground (max. depth 50 m). Water levels were generally measured from ground surface. The density of measurements was insufficient to generate a groundwater contour map. However, an historic groundwater map of the area was obtained from the mining archives, which indicates a hydraulic gradient from east to west.

A clean sampling vessel was used to obtain water samples. Samples from the Tisza River were taken as far from riverbanks as possible and at approximately 0.5 m depth. All equipment was rinsed with the water to be sampled prior to each measurement and sampling. A bailer attached to a 200 m cable was used for depth specific water sampling in the mine craters and mine shafts. The bailer was lowered to the desired sampling depth when a slider was released, activating a mechanism to capture the water at that depth inside the bailer. In total, 30 water samples were taken in 30 mL brown glass bottles. These samples were sent to Germany (Federal Institute for Geosciences and Natural Resources) and analyzed in less than 10 days after sampling. Analyses included stable isotope composition (^{18}O and ^{2}H) as well as major ions, using Cavity Ring-Down Spectroscopy (CRDS) and Ion Chromatography (IC), respectively (Table A1 in Appendix A). The correlation of EC with Na^+ and Cl^- in Fig. 4 shows that halite dissolution is the dominant process determining EC at Solotvyno. Thus, EC values measured in the field will be taken as a proxy for halite dissolution in the following.

In addition to the hydrogeological survey, measurements of chloride concentrations were obtained for several stations in Hungary and Ukraine from the respective authorities (i.e. Central Direction for Water and Environment, Hungary and State Ecological Inspectorate of Ukraine). Satellite images were used for surface observations and geological mapping was conducted in the field.

2. Results and discussion

Images of the mine craters overlying Mine No 7 and Mine No 8 are shown in Fig. 5 for the years 2012 and 2016. These craters have an approximate diameter of 250 m. Mine No 7 seems relatively stable, as the diameter did not change significantly between 2012 and 2016, even though a rise in water level might give the impression of change at the first glance. Taking into account crater wall steepness a slow growth in both southern and north-western directions can be noticed. Measurements of the 28 m deep Crater

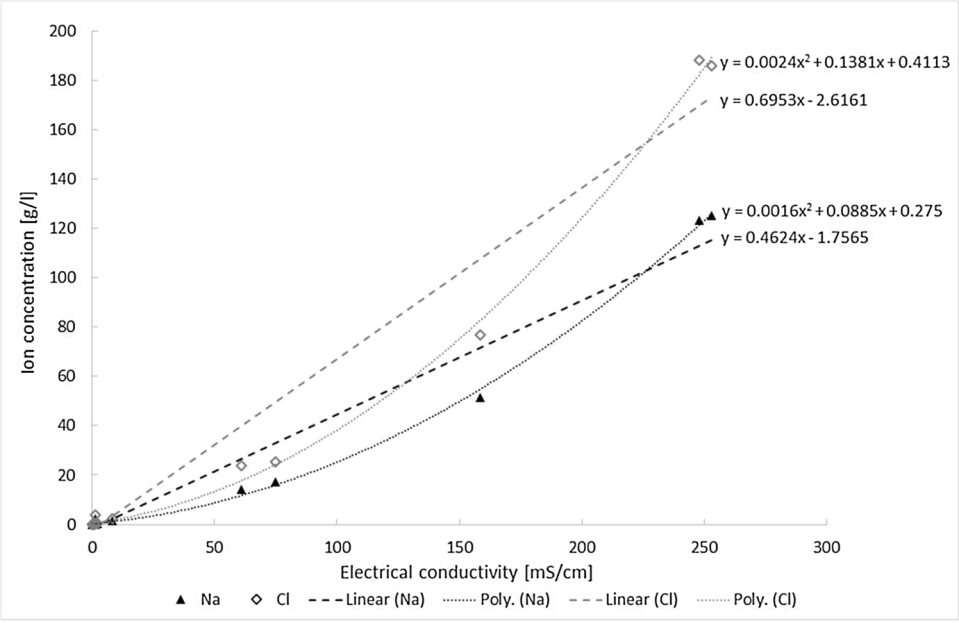

Fig. 4. Linear (dashed) and polynomic (dotted) correlation and respective trend line equations between electrical conductivity [mS/cm] and ion concentration [g/l] (Na^+ in grey and Cl^- in black).

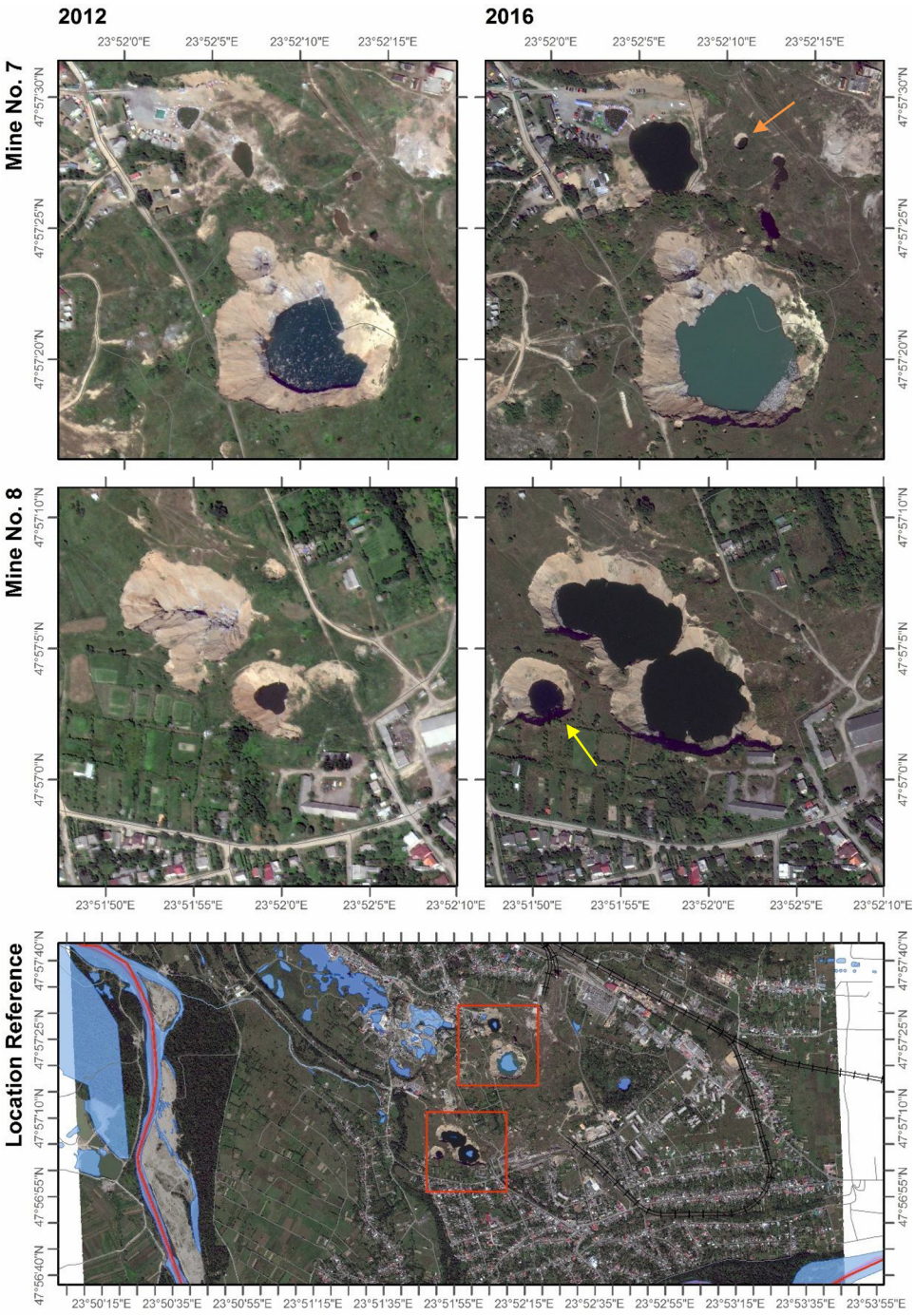

Fig. 5. Aerial view for comparison of craters at Mine No 7 and No 8 in 2012 and 2016. In the lower figure, the reference location for Mine No 7 and No 8 (upper and lower red square, respectively) are shown (google earth©). Orange and yellow arrows indicate location of recent collapses/sinkholes.

Lake above Mine No 7 were conducted during this study and show salinity values resembling saturated brine, i.e. EC of 250 mS/cm (Fig. 6). This collapse thus seems to be in equilibrium, i.e. no further dissolution will take place (as long as no other fresh water sources are present here). At Mine No 8, which collapsed in 2010 as a result of flooding, an increase in crater volume can be observed from the satellite images: The two larger craters show a connection in 2016. Additionally, a new crater appeared south west of the larger craters after 2012 (yellow arrow in Fig. 5), reflecting the developing situation and potential for further collapses in this region (Daupley et al., 2018). Consequently, health and safety dictated that the crater lake associated with Mine No 8 should not be sampled. Mine Shaft No 8, located approximately 70 m east of the collapses was sampled instead. Here, the groundwater level was found to be 33 m below ground level. The EC was around 50–60 mS/cm in the upper 13 m, showing a rapid increase to near saturation of around

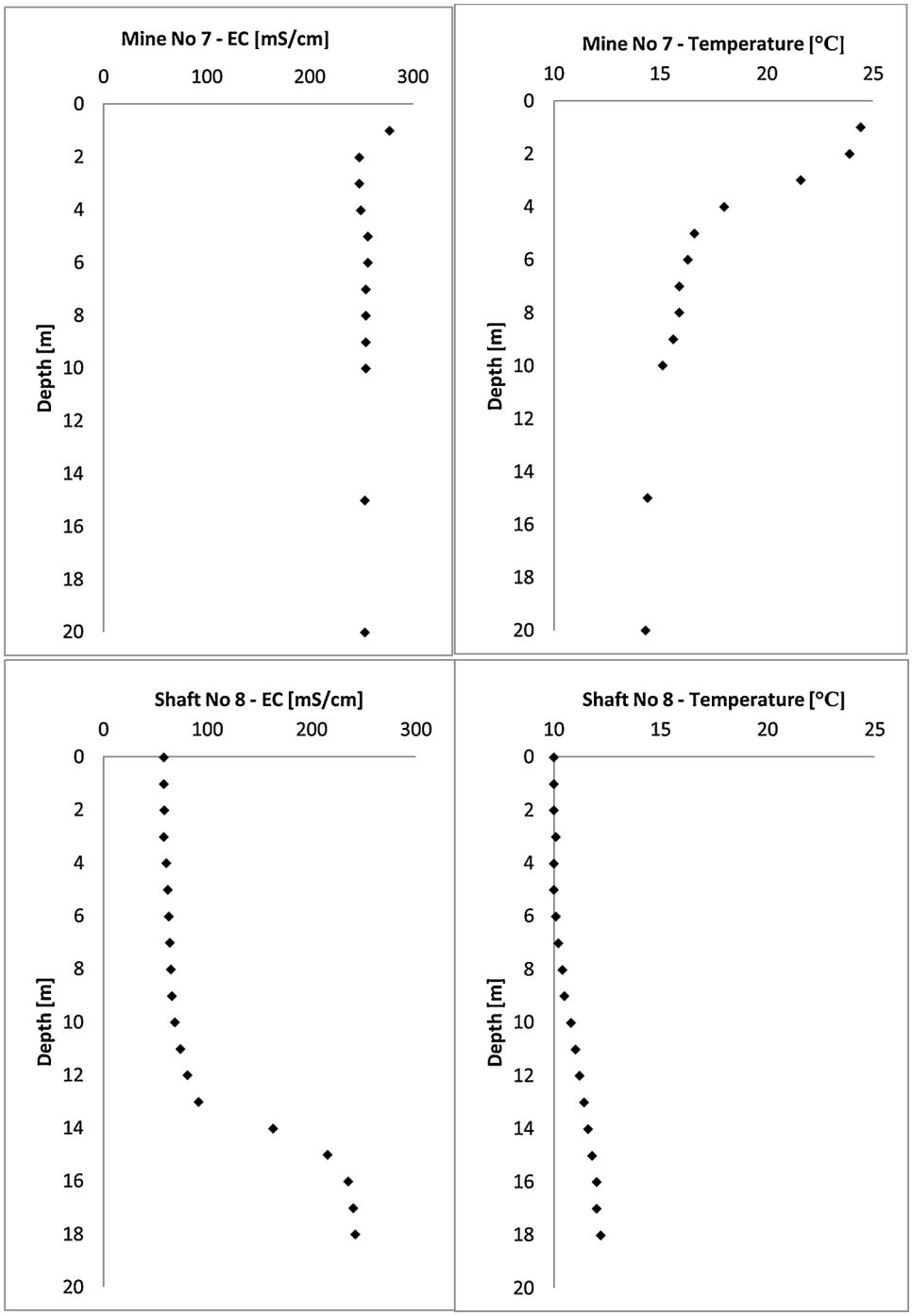

Fig. 6. Electrical conductivity [mS/cm] and temperature [°C] profiles at the Crater Lake of Mine No 7 (above) and Mine Shaft No 8 (below).

240 mS/cm over only a few metres (Fig. 6). This increase in mineralization at around 40 m below ground roughly corresponds to the depth of the salt dome on its southern flank, in the vicinity of Mine No 8. Thus, the thickness of the unsaturated zone at Shaft 8 (Mine No 8) roughly corresponds to that of the Quaternary sediments above the water level of Mine Crater No 7. Such high electrical conductivities of more than 10 mS/cm are only found at the two locations a) the Mine Crater of Mine No 7 and b) the Mine Shaft of Mine No 8. The northern drainage system (west of Lake Solotvyno, coordinates provided in Table A1 in Appendix A) shows moderate elevation in EC of 8180 µS/cm, proving that water from the mine is continually draining into the Tisza River.

The main mining shaft of Mine No 9 (north of the salt dome) was not accessible for safety reasons. The so called “skip shaft” around 200 m farther north, originally used for material transportation, was sampled instead. Its depth is understood to be 525 m, however only the lower 30 m penetrated the salt dome (personal communication with former mining staff). The groundwater level

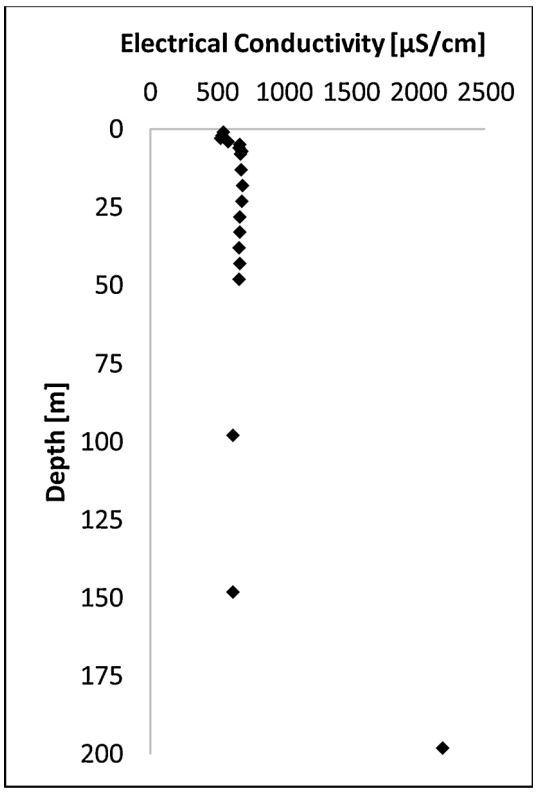

Fig. 7. EC [µS/cm] profile at Mine Shaft No 9 (shaft) up to a depth of 198 m below ground surface.

was found to be 2 m below the ground surface. An EC signal of around 650 µS/cm indicated fresh water in all measurements taken. Slight mineralization (EC of 2180 µS/cm) and a strong red colour (probably resulting from iron dissolution of the shaft construction) was found only in the deepest sample taken at a depth of 198 m (

Fig. 7). Temperature decreased from 15 °C to a constant value of around 12 °C within the first eight metres of the water column.

A sinkhole of approximately 7 m depth was reported to have collapsed on May 2nd 2016 (hereafter 2-May-2016 Sinkhole; orange arrow in Fig. 5). This collapse represents the most recent event in the area at the time of this study. The sinkhole is located between Mine No 7 and Mine No 9 and contains water with a depth of approximately 3 m with saline to hyper-saline characteristics, i.e. EC values between 49 and 116 mS/cm (see Table 1). Temperature seems to increase strongly from 19.1 °C to 25.6 °C within the first metre. This is assumed, however, to be the result of a cold bailer when water sampling was started, which was subsequently warmed up by the relatively warm water in the sinkhole. Another explanation would be the influence of dropping night temperatures, as sampling was conducted in autumn, which results in the cooling of the uppermost layer of the stagnant water in the sinkhole.

Solotvyno Lake (largest lake, north west of the salt dome) has maintained a lower salinity than Lake Kunigunda (smaller lake, east of Solotvyno Lake) over a period of tens of years according to interviews with locals. This is also reflected in the measurements taken during this mission: a maximum lake depth of 5.8 m was measured, and a clear stratification in electrical conductivity as well as temperature was measured at all 10 monitoring locations, which were evenly spaced over the lake area. Temperature measurements were highest at a depth of about 1–2 m below the surface, while EC increased from saline (30 mS/cm) to hyper-saline (around 100–150 mS/cm) at the maximum depth (Fig. 8). This is comparable with measurements taken by Chonka et al. (2013), who show a general increase of water density over depth. However, they also observed a substantial decrease in total mineralization between the years 1997 and 2001. Their temperature profiles also show a comparable shape, with maximum temperatures at a depth of between 1 m and 4 m, depending on the time of the year when sampling was conducted.

Table 1
Electrical conductivity [µS/cm] and temperature [°C] measurements at "2-May-2016 Sinkhole".

Depth [m]	EC [mS/cm]	Temp. [°C]
0	49.2	19.1
1	74.8	25.6
2	129.7	26.8
3	115.7	24.6

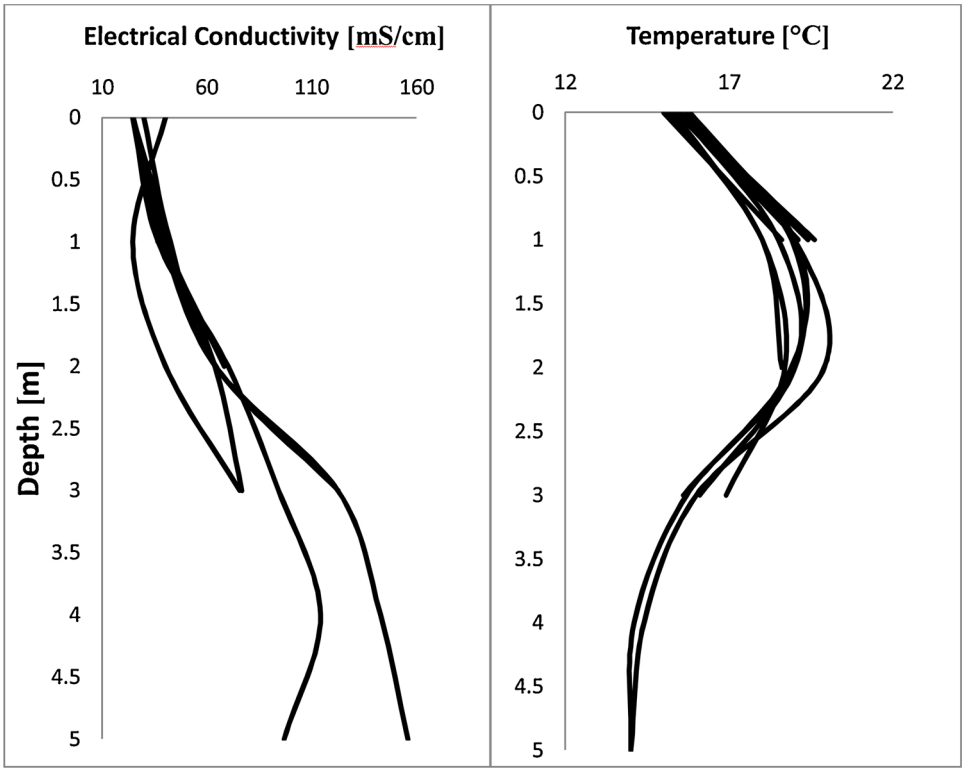

Fig. 8. Ten (similar) EC and temperature profiles taken at different random sampling locations from Solotvyno Lake. Maximum depth at the centre of the lake was 5 m.

Prior to its drainage, the Black Moor area (east of the salt dome, Fig. 2) comprised a mire. From interviews with locals, it is known that the water inside the Black Moor sinkhole, which nowadays is more a lake, suddenly drained, literally overnight, on two historical occasions. A photograph dates one incident to 02.12.2005 (source: mine bureau in Solotvyno). Personal communication, as well as analysis of the margins of the Black Moor sinkhole, further suggest that the whole area subsided more than 10 m. This highly dynamic situation suggests a direct connection either to one of the mines or a karst chamber formed by dissolution. As historical mine maps prove, the Black Moor is not situated directly above one of the mine chambers, however, karst conduits are likely to have developed, connecting the Black Moor sinkhole with one of the mines. It is considered most likely that karst conduit connection was established between the Black Moor sinkhole and Mine No 8, which was still active in 2005 and is much closer to the surface than Mine No 9. In both mines, excessive rates of dewatering might have redirected fresh water flow and led to additional dissolution of rock salt. If one of the pillars of the mines had been weakened and eventually collapsed, sudden drainage of the Black Moor sinkhole could be explained.

Two measurement sites at the centre and the side (east) of Black Moor sinkhole were selected for EC and temperature, as well as for depth specific sampling for chemical and isotopic analyses. The side location (maximum depth of 3.3 m) showed a stable EC of around 1550 μS/cm, over the full depth of the sinkhole and indicative of mineralized fresh water (Fig. 9). The same trend was observed at the central location, however, EC increased over depth and reached its maximum of 3110 μS/cm at 8.3 m below water level. Temperature at the side of the Black Moor sinkhole was significantly lower in the upper three metres (11.9 °C) compared to the central location (17.9 °C). With increased depth the temperature decreased in the central location, reaching its minimum of 10.0 °C at a depth of 8.3 m. As 12 °C was found to be the mean groundwater temperature in this area at other locations sampled, this might indicate active through-flow. Conversely, a lower temperature could also be explained by shading of the sides of the Black Moor sinkhole by vegetation, as indicated by the isotopic analyses (Fig. 10).

Samples for stable isotope analyses were taken from the locations described above and sent to the Federal Institute for Geosciences and Natural Resources (BGR) laboratories for analyses. The composition of stable isotopes varies between different waters due to processes leading to “fractionation” between relatively “heavy” (^{18}O and ^{2}H) and “light” isotopes (^{16}O and ^{1}H). These processes are various, but include evaporation, and depend on geographical as well as meteorological conditions (e.g. distance to ocean, elevation, temperature, evaporation, etc.). A distinct signature of the stable isotope composition between the different end-members (i.e. shallow and deep groundwater, precipitation, and river water) might thus be used to interpret mixing processes of different waters and determine their origin (Clark and Fritz, 1997).

The analytical results have been plotted in relation to the Vienna Mean Standard Ocean Water (VSMOW), and the stable isotope compositions have been discriminated according to the specific sampling locations indicated by the different colours (Fig. 10): mine water from the crater of Mine No 7 and Mine Shaft No 8 (red dots and circles, respectively), as well as water from Mine Shaft No 9, show a distinct evaporation effect, where the red dots of the open water in the crater plots below the Global and Local Meteoric Water

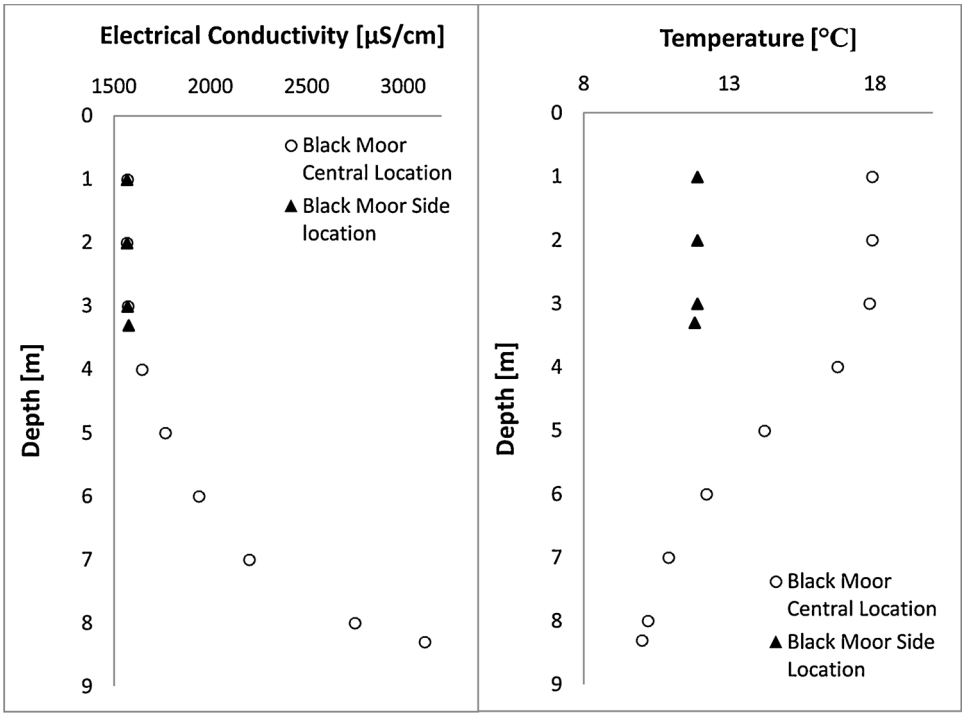

Fig. 9. EC [µS/cm] and temperature [°C] profiles at Black Moor central (circles) and side location (triangles).

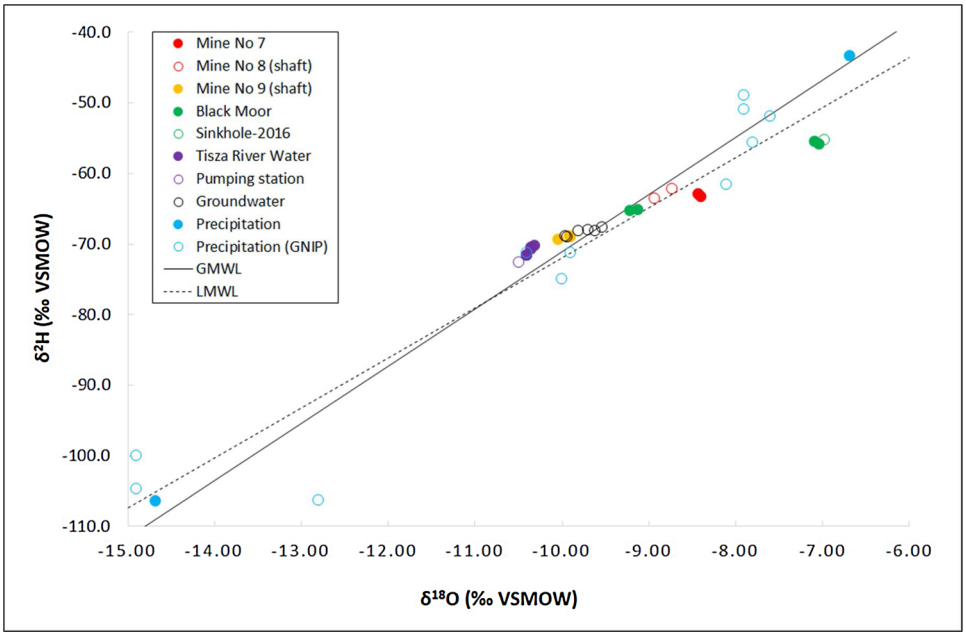

Fig. 10. Dots show measured stable isotopes of $\delta^{18}O$ and $\delta^{2}H$ in relation to Vienna Mean Standard Ocean Water (‰ VSMOW), blue circles show external monthly average data of precipitation from a GNIP station 200 km north of Solotvyno.

Line (GMWL and LMWL as solid and dashed lines, respectively). Fresh water, encountered over a depth of nearly 200 m in Mine Shaft No 9, shows a similar stable isotope signature as that of groundwater in the area (black circles).

Water sampled at the pumping station (purple circle) plots close to water taken from the Tisza River (purple dots) indicating the use of bank filtration water and importance of this zone for public water supply in Solotvyno. This precious fresh water resource contributes drinking water supply not only at Solotvyno, but also further downstream in Romania, Hungary, and Croatia. The isotopic composition of the Tisza River water, on the one hand might be subject to evaporation, but on the other hand clearly carries a "lighter" or "more depleted" isotope composition, which is commonly encountered for groundwater. The fact, that most of the Tisza

River water originates in the high Carpathian Mountains might explain the depletion in "heavy" isotopes here. Further, these values can be explained by the fact that the river was at base-flow conditions during time of sampling in fall (end of dry period), thus mainly fed by discharging groundwater from the Carpathians. Average values of Tisza River water sampled at Sylotvyno (−10,36 ‰ in $\delta^{18}O$ and −70,94 ‰ in $\delta^{2}H$) are in good accordance with measurements taken in August and September 2007 by Rank et al. (2009) at Tiszabecs, at the border between the Ukraine and Hungary (−10,19 ‰ in $\delta^{18}O$ and −70,2 ‰ in $\delta^{2}H$). They compared their data to a previous sampling campaign carried out in March 1988 and recognize a change from spring to autumn discharge of around 1 ‰ in $\delta^{18}O$, which is less surprising when looking at the variability of stable isotopes in precipitation.

Average monthly stable isotope data in precipitation were obtained from GNIP (Global Network for Isotopes in Precipitation, URL-II, 2020), consisting of 35 values measured between 1980 and 1990 at Lwiw, Ukraine, approximately 200 km north of Solotvyno. The spread of this data supports that of the two samples taken during the two last days of the field campaign; the only rainfall that occurred during the period of fieldwork. In isolation, these values cannot be used to define a reliable end member, i.e. identifying specific isotopic composition of local groundwater recharge, which would have helped to further understand the system.

The green dots in (Fig. 10) represent water samples from the Black Moor (at two locations, centre and side). The two samples taken at a depth of 4.5 m and 6.5 m (central location), are located at the GMWL/LMWL ($\delta^{18}O$ of around u-9.2 ‰). In contrast, green dots showing a more "heavy" isotope composition ($\delta^{18}O$ of around -7 ‰) were taken closer to the surface of the Black Moor sinkhole (1.5 m and 2.5 m at central and side location, respectively). The 2-May-2016 Sinkhole exhibits a similar isotopic composition (green circle). These analyses again clearly show the influence of evaporation from the water surface, which leads to fractionation. This means that at the time of sampling, water in the Black Moor can be assumed to have been stagnant, exposing the upper levels to evaporation. The stagnation is also reflected in the density stratification, where water with a higher density (lower temperature and higher EC, see profiles of Fig. 9) underlies a layer of water with a lower density.

When interpreting isotopic signature, tectonic disturbances must also be taken into account; especially on the eastern part of the salt dome structure, where sandstones are fractured, pyritized, and show high quartz content, indicating proximity of the tectonic disturbances. Lines of tectonic disturbances can also be tracked in different parts of salt dome structure which are probably opened by the Tisza drainage gallery (Shekhunova et al., 2015). Such features might lead to flow of, for example, deep confined groundwater, bringing different isotopic end members into the system.

Chemical analyses conducted at the BGR laboratories included cations, anions and minor elements (Table A1 in Appendix A). Fig. 11 shows a Piper diagram of different sampling groups. Due to the limited time during the mission, HCO_3 was back-calculated from the ion balance, thus inaccuracies might be present. However, especially in samples with elevated NaCl content, HCO_3 as residuum was negligible (< 5 % of total anions). The Piper diagram shows that the waters evolve from Na-Cl to $Ca-HCO_3$ types from the centre of the salt dome to the River Tisza. The highest NaCl contents were observed in samples from different depths of the crater of Mine No 7, Shaft of Mine No 8, Kunigunda Lake and the recent 2-May-2016 Sinkhole (red circle in Fig. 11). The Black Moor water (green in Fig. 11) classifies as Na-Cl water type, potentially indicating contact between the Black Moor water and the salt dome, albeit with lower levels of mineralization. Broadly, the waters appear to evolve from Na-Cl types to HCO_3 types with the local hydraulic gradient across the salt dome, i.e. assumed to be from north east to south west, and driven by water originating from the Magura Mountains. Thus, the chemical composition of the water from Mine 9 (orange in Fig. 11) shows values between the "unaffected" groundwater (black in Fig. 11) and the mineralized waters. The pumping station for public water supply was also sampled and the composition is very similar to that of the Tisza water itself, suggesting either dilution away from the centre of the salt dome, or bank filtration. Precipitation with a low mineralization plots at the bottom in the Piper diagram showing a significantly different signature. Unfortunately, neither chemistry nor isotopes serve to differentiate between water originating locally in the Magura Mountains and the regional groundwater flow e.g. originating in the Carpathians.

River quality data provided by the Ukrainian and the Hungarian authorities at the stations Solotvyno and Tyachiv, as well as Tiszabecs, respectively are shown in Fig. 12 (after SEIU, 2016). Whilst data downstream of Solotvyno show elevated salt loads, especially prior to 2008, the station located at Solotvyno does not show high chloride concentrations. The low concentrations are explained by the fact that this monitoring station is situated slightly upstream of the mining area. The data from downstream of Solotvyno show that annual average concentrations of Cl^- have steadily decreased since 2008. This is assumed to be the consequence of the cessation of mining operations and a much smaller input of active drainage into the Tisza as a result of pumping. Alternatively, the collapsed mine chambers, e.g. of Mine No 8, might not yet be completely filled with water and a saturation equilibrium might not be reached. The health and safety limitations on monitoring meant that this could not be verified during the responsive visit. If the latter hypothesis is right, the hydraulic gradient might change once equilibrium is established, with a potential to redirect overflow water towards the Tisza.

Cl^- concentrations that were measured, during the mission, in the Tisza River ranged between 2.89 mg/l (upstream) and 13.5 mg/l (downstream), and did not show any anomalies during this period. The slightly higher Cl^- concentrations downstream correspond with an input from a northern drainage system (Cl^- concentration of 2354 mg/l), which continuously releases dissolved NaCl from the Solotvyno mining area into the Tisza River. SO_4^- and NO_3^- concentrations were low in the river water, although NO_3^- was moderately elevated (between 14.2 and 30.5 mg/l) in a small tributary, the drainage systems and one local water supply well (Table A1 in Appendix A). This is attributed to human activity (e.g. agricultural fertilizers, waste or sewage).

3. Conclusions

Field investigations in September and October 2016 have contributed to the conceptual understanding of the present hydrogeological situation at Solotvyno. The model presented in Fig. 3 was developed with a particular focus on the potential influences of natural and anthropogenic impacts on the Tisza River water quality. It shows several potential flow paths that could discharge saline water derived from contact with the salt dome towards the Tisza River.

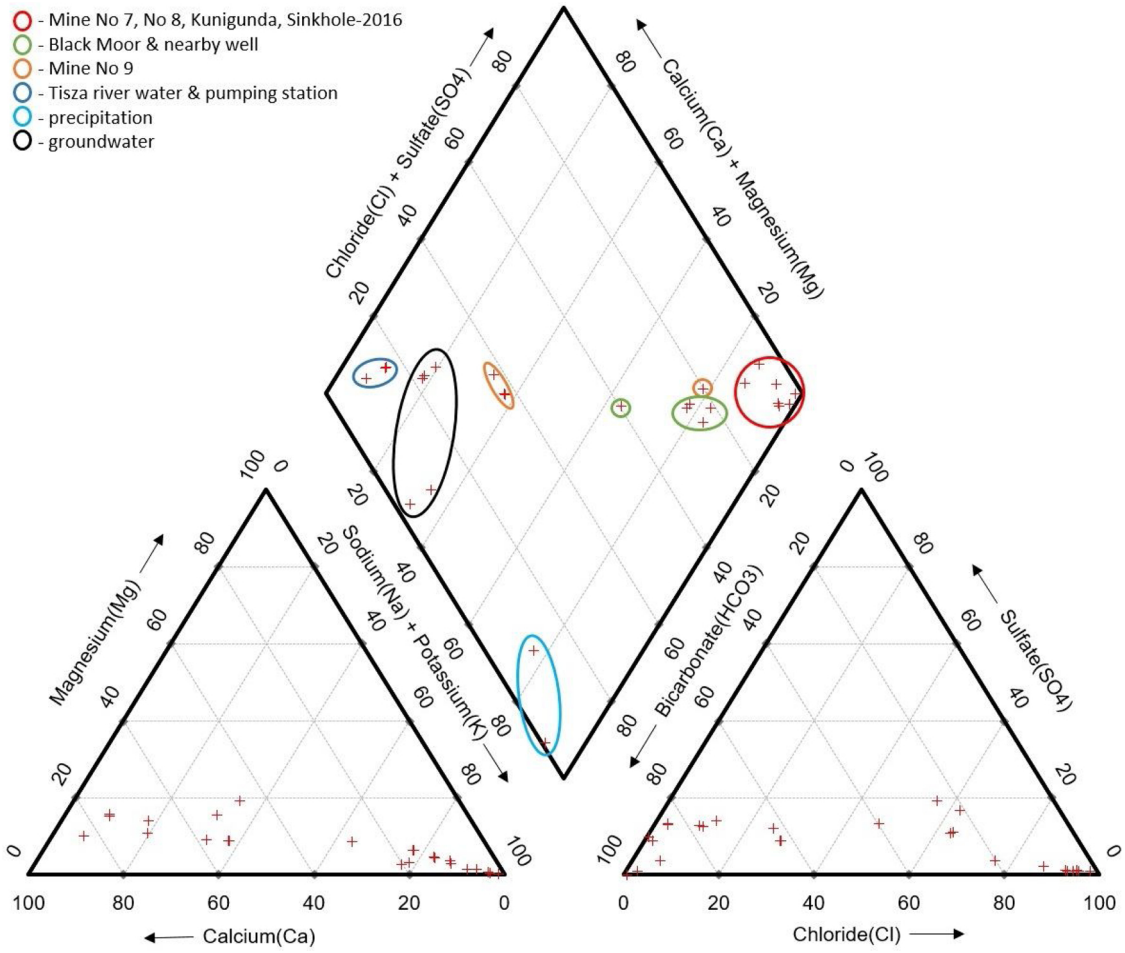

Fig. 11. Piper diagram showing distribution of main ions from different waters at Solotvyno.

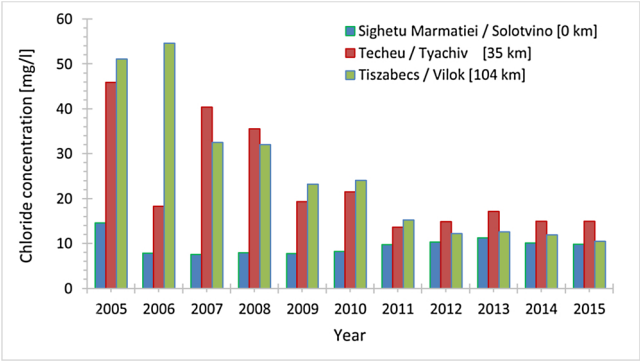

Fig. 12. Annual mean chloride concentrations at three different stations. In blue: at Solotvyno, red: 35 km, and green: 104 km downstream of Solotvyno (source: SEIU, 2016). Note that the station at Sighetu Marmatiei / Solotvyno is situated just upstream of the mining area.

The Black Moor sinkhole was identified as one of the key drivers for dissolutional activity, as a consequence of the north-east to south-west hydraulic gradient, and a hydrological window that might facilitate contact between recharge water and the salt with the potential to cause further dissolution, as it is likely to be in direct contact with underground cavities, e.g. mine chambers. Chemical analyses, i.e. a slightly elevated NaCl signature, suggest that some of the water in the Black Moor was formerly in contact with the salt dome albeit with the addition of large quantities of unsaturated waters. If quickly drained, this water might lead to additional dissolution of rock salt in the subsurface and to changes in pressure gradients resulting in a disturbance of the preliminary equilibrium.

As surface water input is generally small, particularly during low groundwater levels, the potential for contamination by water released from surface water courses, e.g. creeks due to heavy rainfall or the Tisza as a result of flooding, is assumed to be small. In the

extreme case of high river stage, combined with flooding of the former mining area, salt load in the Tisza River would be diluted by the quantity of discharge during such an event. The same is the case for shallow groundwater flow through the Alluvium. Additionally, groundwater closer to the Tisza River, e.g. in the Alluvium of the southern part of the salt dome measured in Shaft No 8, was not completely salt saturated in the near surface (compare Fig. 5). Even though hyper-saline waters are present in the main craters and at the lakes, these waters are not likely to be discharged into the Tisza, as they are a) protected by a thick layer of Alluvium in the case of the craters, b) protected by a flood barrier in the case of the lakes, and c) generally protected by a layer of Pallag (residual clay) in the rest of the former mining area. The relatively impermeable Pallag layer, which is actively forming in some areas, acts as a protective layer minimizing the potential for further dissolution of the surface of the salt.

At high river stages of the Tisza River, i.e. during flood events (or due to seasonal changes), pressure gradients in the Alluvium of the Solotvyno mine area might change. This is the case for the flood plains of the Tisza River, possibly leading to a mobilization of saline water stored here. Especially after an extended dry period of several years where saltwater may accumulate, the mobilization of saline water might lead to sudden saline input into the Tisza River prior to a flooding event. This potential scenario suggests the need for the installation of a monitoring system to a) better understand the system through long term measurements and b) to minimize reaction times for adequate control measures.

There is a small possibility that flow from the ancient mine drainage systems towards the Tisza could be resumed with a potential to discharge larger quantities of salt water. However, for this situation to develop, the pressure gradient would need to be modified by raising the head with additional water. Moreover, it was observed that these drainage systems have not been maintained and are broken at different locations, restricting flow in the tunnels and aqueducts.

The conceptual model shows that the surface of the salt dome is generally protected by a layer of Pallag. There are a number of scenarios that might lead to the disturbance of this layer (e.g. the drilling of boreholes, new constructions or the collapse of abandoned workings. Furthermore, the process of dissolution might be enhanced by the presence of leachate derived from waste disposal, as well as any renewed exploration for salt extraction that involves constructing new mine shafts. Therefore, there is a requirement that these activities could be limited by careful planning and land management.

Although upwelling of deep, salt contaminated groundwater might occur via cracks, faults, or discontinuities in the bedrock during flooding and high groundwater conditions, flow velocities are likely to be much smaller than those of overland or alluvial flow, thus dilution would likely mask any impact. Furthermore, no such inputs were detected from a longitudinal profile of EC along the 14 km stretch of the Tisza gathered during the hydrogeological survey.

The findings indicate a requirement for ongoing monitoring of discharge and water quality of the River Tisza, both upstream and downstream of Solotvyno, as well as of existing wells, drainage systems, and creeks between the mining area and the river. However, care will be required in the design and installation of any new monitoring or investigation boreholes, which otherwise might lead to undesired consequences with the possibility of forming new hydrological windows and potential flow paths leading to fresh water contact with the salt dome, and consequential dissolution processes. Similarly, all anthropogenic activity in the area should meet strict technical standards. The flood protection dam is another source of vulnerability and the infrastructure associated with this hydraulic structure should be the subject of further research, specifically the drainage galleries, e.g. the remains of the Tisza drainage gallery, which protects the north-eastern part of the salt dome structure from significant water inflow and need to be maintained in working order.

In conclusion, the risk of salt pollution of the Tisza River from the abandoned Solotvyno mines is considered to be low at the time of the visit. However, given the proximity of such a large quantity of saline groundwater to the river, a strong recommendation was to design and implement a monitoring programme. A further recommendation was the extension of the protection zone around the mining area to both protect the civil population and reestablish a stable situation in the groundwater by minimizing potential surface water ingress and disturbance of the saline water column.

CRediT authorship contribution statement

Leonard Stoeckl: Software, Investigation, Validation, Conceptualization, Writing - review & editing. **Vanessa Banks:** Software, Investigation, Validation, Conceptualization, Writing - review & editing. **Stella Shekhunova:** Software, Investigation, Validation, Conceptualization, Writing - review & editing. **Yevgeniy Yakovlev:** Software, Investigation, Validation, Conceptualization.

Declaration of Competing Interests

The authors declare that they have no known competing financial interests or personal relationships that could have appeared to influence the work reported in this paper.

Acknowledgements

The European Commission and the Emergency Response Coordination Centre (ERCC) are acknowledged for the possibility of this mission, the mining bureau in Solotvyno for their open and constructive cooperation. We further thank the Ukrainian State Rescue Team for measurements and sampling at locations with difficult access, the Hungarian and Ukrainian authorities for providing Tisza river data, and BGR laboratories for their effort in rapid isotope and chemistry analyses. VB publishes with the permission of the Executive Director of the British Geological Survey.

Appendix A

Table A1
Groundwater analysis data.

Sample number	Date of sampling	Water type	Sampling location	Latitutde [decimal degrees]	Longitude [decimal degrees]	Temperature during sampling [°C]	pH [-]	Electrical conductivity [µS/cm]
EUCPT001	20.09.2016	groundwater	Private well	47,970235	23,876301	11,3	6,91	869
EUCPT002	20.09.2016	groundwater	Groundwater spring	47,973841	23,861185	11,3	7,21	439
EUCPT004	20.09.2016	reservoir	Pumping Station reservoir	-	-	15,8	7,3	442
EUCPT005	20.09.2016	groundwater	Public supply well (shaft)	47,951310	23,860485	14	7,07	718
EUCPT007	20.09.2016	surface water	River Tisza (Location 1)	47,944217	23,844303	16,5	8,3	275
EUCPT009	21.09.2016	groundwater	Well near black moor	47,956218	23,877595	13,62	7,07	1279
EUCPT010	21.09.2016	groundwater	South drainage system	47,943916	23,881435	12,4	-	670
EUCPT011	21.09.2016	surface water	River Tisza (Location 2)	47,942911	23,880003	15,4	-	262
EUCPT012	21.09.2016	groundwater	North drainage system	47,962015	23,856783	12,9	-	8180
EUCPT013	23.09.2016	surface water	Black moor side location (1.5 m b.s.)	47,954661	23,878837	11,9	-	1565
EUCPT014	23.09.2016	surface water	Black moor center (1.5 m b.s.)	47,954507	23,878558	17,9	-	1565
EUCPT015	23.09.2016	surface water	Black moor center (4.5 m b.s.)	47,954507	23,878558	15	-	1700
EUCPT016	23.09.2016	surface water	Black moor center (6.5 m b.s.)	47,954507	23,878558	11,5	-	2000
EUCPT019	24.09.2016	surface water	Mine#7 (2 m b.s.)	47,955753	23,869499	23,9	6,4	248000
EUCPT021	24.09.2016	surface water	Mine#7 (16 m b.s.)	47,955753	23,869499	14,4	6,07	253000
EUCPT022	24.09.2016	surface water	2May2016_Sinkhole	47,957882	23,869803	26,8	6,76	130000
EUCPT023	24.09.2016	groundwater	Mine9_Shaft10 (98 m b.s.)	47,960204	23,873616	12,5	7,86	615
EUCPT024	24.09.2016	groundwater	Mine9_Shaft10 (148 m b.s.)	47,960204	23,873616	12,5	7,84	615
EUCPT025	24.09.2016	groundwater	Mine9_Shaft10 (198 m b.s.)	47,960204	23,873616	12,5	7,82	2180
EUCPT026	25.09.2016	groundwater	Mine8_Shaft8 (150 m b.s.)	47,950933	23,870509	14	7	158500
EUCPT027	25.09.2016	groundwater	Mine8_Shaft8 (38 m b.s.)	47,950933	23,870509	11,4	7,25	61000
EUCPT029	29.09.2016	surface water	River Tisza (Loc. 3)	47,986460	23,672246	16,7	-	342
EUCPT030	29.09.2016	surface water	River Tisza (Loc.4)	47,966004	23,835891	16,2	-	330
EUCPT031	29.09.2016	surface water	Small contributary (Glod)	47,966650	23,837141	13,9	-	1265
EUCPT037	03.10.2016	rain water	Base of Operation (a)	47,970788	23,858310	-	-	-
EUCPT038	05.10.2016	rain water	Base of Operation (b)	47,970788	23,858310	-	-	-

(values with "<" indicate measurements below detection limit)

Sample number	K [mg/l]	Na [mg/l]	Cl [mg/l]	Mg [mg/l]	Ca [mg/l]	SO4 [mg/l]	Fe(II) [mg/l]	Mn [mg/l]	NO3 [mg/l]	Br [mg/l]	NO2 [mg/l]	F [mg/l]
EUCPT001	4,7	76,6	9,20	19,6	110	4,41	< 0.03	0,31	0,20	< 0.03	0,13	0,12
EUCPT002	1,0	39,3	10,2	11,7	45,5	8,87	< 0.03	0,01	2,41	< 0.03	< 0.03	0,06
EUCPT004	2,6	7,6	3,07	6,15	83,4	21,3	< 0.03	< 0.01	3,02	< 0.03	< 0.03	< 0.03
EUCPT005	10,9	34,6	33,5	10,3	107	51,1	< 0.03	< 0.01	25,3	< 0.03	< 0.03	0,03
EUCPT007	1,6	6,5	2,97	5,63	45,8	19,2	0,03	< 0.01	1,39	< 0.03	< 0.03	0,03
EUCPT009	2,7	181	207	12,9	68,7	79,8	< 0.03	2,16	0,03	< 0.03	< 0.03	0,05
EUCPT010	4,6	50,4	56,4	7,35	77,6	37,5	< 0.03	0,01	30,5	< 0.03	< 0.03	0,05
EUCPT011	1,3	6,3	2,89	5,68	45,1	19,1	0,03	< 0.01	1,33	< 0.03	< 0.03	0,03
EUCPT012	4,4	1520	2354	33,6	147	76,4	< 0.03	0,01	15,9	< 0.03	< 0.03	0,11
EUCPT013	4,0	258	325	11,0	46,3	76,2	0,33	0,01	0,50	< 0.03	0,68	0,09
EUCPT014	4,0	254	323	10,8	45,2	77,0	0,33	0,01	0,30	< 0.03	0,86	0,09
EUCPT015	3,8	310	325	9,33	39,8	152	3,02	3,51	0,80	< 0.03	6,78	0,16
EUCPT016	4,2	382	445	11,8	49,7	162	5,73	5,83	0,03	< 0.03	0,20	0,12
EUCPT019	51,9	123300	188000	86,4	1310	2430	< 0.3	8,1	3	5	< 3	< 3
EUCPT021	49,7	125100	185800	79,2	1240	2280	< 0.3	8,4	4	4	< 3	< 3
EUCPT022	15,9	17190	25260	43,0	424	437	< 0.3	4,8	6	< 3	< 3	< 3
EUCPT023	3,2	56,8	66,9	7,03	70,1	27,8	0,05	0,02	2,30	< 0.03	< 0.03	< 0.03
EUCPT024	3,0	55,6	65,6	6,98	69,3	27,7	< 0.03	< 0.01	2,29	< 0.03	< 0.03	< 0.03
EUCPT025	3,3	362	543	7,42	73,9	35,2	< 0.03	< 0.01	2,37	< 0.03	< 0.03	< 0.03
EUCPT026	42,7	51470	76610	211	1410	1050	1,2	6,6	< 3	< 3	< 3	< 3
EUCPT027	27,0	14230	23650	248	1400	300	< 0.3	5,2	4	< 3	< 3	< 3
EUCPT029	2,1	15,7	12,7	6,33	50,7	23,1	< 0.03	< 0.01	1,82	< 0.03	< 0.03	0,03
EUCPT030	2,0	15,4	13,5	6,16	49,5	22,3	< 0.03	< 0.01	1,66	< 0.03	< 0.03	0,03
EUCPT031	10,5	2360	3687	18,7	114	65,6	< 0.03	< 0.01	14,2	0,09	0,35	0,09
EUCPT037	0,4	3,5	0,05	0,06	0,82	1,19	< 0.03	< 0.01	0,38	< 0.03	0,03	< 0.03
EUCPT038	0,3	3,0	0,05	0,02	0,25	0,09	< 0.03	< 0.01	0,39	< 0.03	0,04	< 0.03

(values with "<" indicate measurements below detection limit)

(*continued on next page*)

Table A1 (*continued*)

Sample number	PO4 [mg/l]	Al [mg/l]	As [mg/l]	BO2 [mg/l]	Ba [mg/l]	Be [mg/l]	[mg/l]Cd	Co [mg/l]	Cr [mg/l]	Cu [mg/l]	Li [mg/l]	Ni [mg/l]
EUCPT001	< 0.3	< 0.03	< 0.2	0,4	0,45	< 0.01	< 0.02	< 0.03	< 0.03	< 0.03	0,04	< 0.03
EUCPT002	< 0.3	< 0.03	< 0.2	0,1	0,09	< 0.01	< 0.02	< 0.03	< 0.03	< 0.03	< 0.03	< 0.03
EUCPT004	< 0.3	< 0.03	< 0.2	< 0.1	0,06	< 0.01	< 0.02	< 0.03	< 0.03	< 0.03	< 0.03	< 0.03
EUCPT005	< 0.3	< 0.03	< 0.2	0,2	0,11	< 0.01	< 0.02	< 0.03	< 0.03	< 0.03	< 0.03	< 0.03
EUCPT007	< 0.3	0,04	< 0.2	< 0.1	0,04	< 0.01	< 0.02	< 0.03	< 0.03	< 0.03	< 0.03	< 0.03
EUCPT009	< 0.3	< 0.03	< 0.2	0,3	0,52	< 0.01	< 0.02	< 0.03	< 0.03	< 0.03	0,05	< 0.03
EUCPT010	< 0.3	< 0.03	< 0.2	0,1	0,11	< 0.01	< 0.02	< 0.03	< 0.03	< 0.03	< 0.03	< 0.03
EUCPT011	< 0.3	0,05	< 0.2	0,1	0,04	< 0.01	< 0.02	< 0.03	< 0.03	< 0.03	< 0.03	< 0.03
EUCPT012	< 0.3	< 0.03	< 0.2	0,9	0,19	< 0.01	< 0.02	< 0.03	< 0.03	< 0.03	0,06	< 0.03
EUCPT013	< 0.3	< 0.03	< 0.2	0,9	0,12	< 0.01	< 0.02	< 0.03	< 0.03	< 0.03	< 0.03	< 0.03
EUCPT014	< 0.3	< 0.03	< 0.2	0,9	0,11	< 0.01	< 0.02	< 0.03	< 0.03	< 0.03	< 0.03	< 0.03
EUCPT015	0,7	1,29	< 0.2	1,4	0,11	< 0.01	< 0.02	< 0.03	< 0.03	< 0.03	< 0.03	< 0.03
EUCPT016	1,6	1,73	< 0.2	1,6	0,13	< 0.01	< 0.02	< 0.03	< 0.03	< 0.03	< 0.03	< 0.03
EUCPT019	< 3	< 0.3	< 2	3,8	1,0	< 0.1	< 0.2	< 0.3	< 0.3	< 0.3	< 0.3	< 0.3
EUCPT021	< 3	< 0.3	< 2	3,5	0,9	< 0.1	< 0.2	< 0.3	< 0.3	< 0.3	< 0.3	< 0.3
EUCPT022	< 3	< 0.3	< 2	< 1	1,3	< 0.1	< 0.2	< 0.3	< 0.3	< 0.3	< 0.3	< 0.3
EUCPT023	< 0.3	< 0.03	< 0.2	0,1	0,05	< 0.01	< 0.02	< 0.03	< 0.03	< 0.03	< 0.03	< 0.03
EUCPT024	< 0.3	< 0.03	< 0.2	0,1	0,05	< 0.01	< 0.02	< 0.03	< 0.03	< 0.03	< 0.03	< 0.03
EUCPT025	< 0.3	< 0.03	< 0.2	< 0.1	0,05	< 0.01	< 0.02	< 0.03	< 0.03	< 0.03	< 0.03	< 0.03
EUCPT026	< 3	< 0.3	< 2	2,1	1,3	< 0.1	< 0.2	< 0.3	< 0.3	< 0.3	< 0.3	< 0.3
EUCPT027	< 3	< 0.3	< 2	< 1	1,6	< 0.1	< 0.2	< 0.3	< 0.3	< 0.3	< 0.3	< 0.3
EUCPT029	< 0.3	< 0.3	< 0.2	< 0.1	0,04	< 0.01	< 0.02	< 0.03	< 0.03	< 0.03	< 0.3	< 0.03
EUCPT030	< 0.3	< 0.3	< 0.2	0,2	0,04	< 0.01	< 0.02	< 0.03	< 0.03	< 0.03	< 0.3	< 0.03
EUCPT031	< 0.3	< 0.3	< 0.2	0,4	0,15	< 0.01	< 0.02	< 0.03	< 0.03	< 0.03	< 0.03	< 0.03
EUCPT037	< 0.3	< 0.3	< 0.2	< 0.1	0,00	< 0.01	< 0.02	< 0.03	< 0.03	< 0.03	< 0.03	< 0.03
EUCPT038	< 0.3	< 0.3	< 0.2	< 0.1	0,00	< 0.01	< 0.02	< 0.03	< 0.03	< 0.03	< 0.03	< 0.03

(values with "<" indicate measurements below detection limit)

Sample number	Pb [mg/l]	Sc [mg/l]	SiO2 [mg/l]	Sr [mg/l]	Ti [mg/l]	V [mg/l]	Zn [mg/l]	d18O [‰ VSMOW]	d18O sd [‰ VSMOW]	d2H [‰ VSMOW]	d2H sd [‰ VSMOW]	D excess [‰ VSMOW]
EUCPT001	< 0.2	< 0.01	20,0	0,61	< 0.01	< 0.03	< 0.03	-9,96	0,06	-69	0,3	11
EUCPT002	< 0.2	< 0.01	36,1	0,26	< 0.01	< 0.03	< 0.03	-9,8	0,09	-68,2	0,2	10
EUCPT004	< 0.2	< 0.01	9,1	0,28	< 0.01	< 0.03	< 0.03	-10,49	0,02	-72,7	0,2	11
EUCPT005	< 0.2	< 0.01	11,5	0,34	< 0.01	< 0.03	< 0.03	-9,94	0,06	-69,1	0,2	10
EUCPT007	< 0.2	< 0.01	6,0	0,18	< 0.01	< 0.03	< 0.03	-10,31	0,1	-70,3	0,2	12
EUCPT009	< 0.2	< 0.01	17,6	0,59	< 0.01	< 0.03	< 0.03	-9,53	0,18	-67,7	0,3	9
EUCPT010	< 0.2	< 0.01	16,1	0,29	< 0.01	< 0.03	< 0.03	-9,61	0,12	-68,2	0,5	9
EUCPT011	< 0.2	< 0.01	6,5	0,18	< 0.01	< 0.03	< 0.03	-10,35	0,11	-70,5	0,2	12
EUCPT012	< 0.2	< 0.01	18,1	1,66	< 0.01	< 0.03	< 0.03	-9,69	0,08	-68,1	0,2	9
EUCPT013	< 0.2	< 0.01	5,2	0,73	< 0.01	< 0.03	< 0.03	-7,04	0,08	-55,9	0,1	0
EUCPT014	< 0.2	< 0.01	5,3	0,72	< 0.01	< 0.03	0,03	-7,09	0,05	-55,6	0,2	1
EUCPT015	< 0.2	< 0.01	19,1	0,60	0,02	< 0.03	0,05	-9,21	0,02	-65,3	0,1	8
EUCPT016	< 0.2	< 0.01	23,6	0,74	0,03	< 0.03	0,11	-9,13	0,09	-65,2	0,4	8
EUCPT019	< 2	< 0.1	< 10	18,5	< 0.1	< 0.3	0,3	-8,42	0,07	-63,0	0,1	4
EUCPT021	< 2	< 0.1	< 10	16,8	< 0.1	< 0.3	0,4	-8,39	0,05	-63,4	0,2	4
EUCPT022	< 2	< 0.1	< 10	6,0	< 0.1	< 0.3	< 0.3	-6,97	0,09	-55,4	0,2	0
EUCPT023	< 0.2	< 0.01	8,9	0,38	< 0.01	< 0.03	< 0.03	-10,04	0,08	-69,4	0,3	11
EUCPT024	< 0.2	< 0.01	8,9	0,38	< 0.01	< 0.03	< 0.03	-9,90	0,04	-69,0	0,3	10
EUCPT025	< 0.2	< 0.01	8,8	0,53	< 0.01	< 0.03	< 0.03	-9,91	0,10	-68,9	0,4	10
EUCPT026	< 2	< 0.1	< 10	13,1	< 0.1	< 0.3	0,3	-8,92	0,05	-63,7	0,2	8
EUCPT027	< 2	< 0.1	10,0	8,0	< 0.1	< 0.3	< 0.3	-8,73	0,04	-62,2	0,2	8
EUCPT029	< 0.2	< 0.01	5,2	0,20	< 0.01	< 0.03	< 0.3	-10,35	0,07	-70,7	0,1	7
EUCPT030	< 0.2	< 0.01	5,6	0,19	< 0.01	< 0.03	< 0.3	-10,40	0,10	-71,6	0,1	7
EUCPT031	< 0.2	< 0.01	11,2	1,14	< 0.01	< 0.03	< 0.3	-7,56	0,07	-56,4	0,2	7
EUCPT037	< 0.2	< 0.01	0,0	0,00	< 0.01	< 0.03	0,10	-6,69	0,16	-43,4	0,6	7
EUCPT038	< 0.2	< 0.01	0	0	< 0.01	< 0.03	< 0.3	-14,68	0,11	-106,4	0,3	6

(values with "<" indicate measurements below detection limit)

Appendix B. Supplementary data

Supplementary material related to this article can be found, in the online version, at doi:https://doi.org/10.1016/j.ejrh.2020.100701.

References

Ashrafianfar, N., Hebel, H.-P., Busch, W., 2011. Monitoring of mining induced land subsidence – differential SAR interferometry and persistent scatterer interferometry using TerraSAR-X data in comparison with ENVISAT data. In: 4th TerraSAR-X Science Team Meeting. February 2011. DLR, Oberpfaffenhofen, Germany. pp. 14–16.

Bukowski, K., Czapowski, G., Karoli, S., Bąbel, M., 2007. Sedimentology and geochemistry of the Middle Miocene (Badenian) salt-bearing succession from East Slovakian Basin (Zbudza formation). In: In: Schreiber, B.C., Lugli, S., Babel, M. (Eds.), Evaporites Through Space and Time 285. Geological Society, London, pp. 309–334 Special Publications.

Chonka, Y., Lemko, I., Sichka, M., Buleza, B., Yarosh, V., Tzoma, I., Sharkan, I., Shevchuk, A., 2013. Physico-chemical and microbiological monitoring of Solotvino Salt Lakes. Balneo Res. J. 4 (3). https://doi.org/10.12680/balneo.2013.1050. September 2013.

Clark, I.D., Fritz, P., 1997. Environmental Isotopes in Hydrogeology. CRC Press/Lewis Publishers, Boca Raton, FL, pp. 328.

Daupley, X., Banks, V., Stoeckl, L., 2018. Review of ground movements as a result of salt mines flooding in solotvyno, Ukraine. In: Proceedings of the Saltmech IX Conference. Sept. 12-14 2018, Hannover, Germany.

Frolov, M.V., 1973. Report: Preliminary Exploration of Natural Brines Solotvino Rock Salt Deposit in the 1971-1973. Geoinform Ukrainy.

Glushko, V.V., 1968. Tectonics and Oil-and Gas Bearing of the Carpathians and Adjoining Throughs. Nedra, Moskow, pp. 264 in Russian.

Gordienko, V.V., Gordienko, I.V., Zavgorodnya, O.V., Logvinov, I.M., Tarasov, V.N., 2012. Evolution of tectonosphere of the Ukrainian Carpathians. Geofiz. Zhurnal 34 (6), 160–178 in Ukranian.

Kutas, R.I., 2014. Heat flow and geothermal crustal model of the Ukrainian Carpathians. Geofiz. Zhurnal 36 (6), 3–27 in Ukranian.

Lide, D.R., 2004. CRC Handbook of Chemistry and Physics, 84th edition. CRC Press LLC, New York, pp. 2616.

OECD, 2008. Surface Water Quality Regulation in EECCA Countries: Directions for Reform. EAP Task Force, pp. 13.

OLHGC, 2009. Official Letter to the Hungarian Governmental Commissioner Authorized for Cross-Border Water Issues between Hungary and Ukraine on the on-Site Mission in Solotvyno, in the Subject of Salt Contamination of the Tisza River 15 May 2009.

Onencan, A., Meesters, K., Van de Walle, B., 2018. Methodology for participatory GIS risk mapping and citizen science for Solotvyno Salt Mines. Remote Sens. 10 (11), 1828. https://doi.org/10.3390/rs10111828. 2018.

Rank, D., Papesch, W., Heiss, G., Tesch, R., 2009. Isotopic composition of river water in the Danube Basin - results from the Joint Danube Survey 2 (2007). Austrian J. Earth Sci. 102 (2), 170–180.

SEIU, 2016. State Ecological Inspectorate of Ukraine; State Ecological Inspectorate of Zakarpat Region 14 Uzhgorod, Shwabska.

Shekhunova, S.B., Aleksieienkova, M.V., Stadnichenko, S.M., Siumar, N.P., 2015. The Integrated Geological Model of Solotvyno Structure as a Tool to Assess Geoecological Sustainability of Solotvyno Rocksalt Deposit 8. Collection of Scientific Works of the Institute of Geological Sciences NAS of Ukraine, pp. 233–250. https://doi.org/10.30836/igs.2522-9753.2015.146791.

Starostenko, V., 2015. Studies of Modern Geodynamics of Ukrainian Carpathians. Naukova dumka, Kyiv, pp. 256 in Ukrainian.

Starostenko, V., Janik, T., Kolomiyets, K., Czuba, W., Sroda, P., Lysynchuk, D., Grad, M., Kovács, I., Stephenson, R., Thybo, H., Artemieva, I.M., Omelchenko, V., Gintov, O., Kutas, R., Gryn, D., Guterch, A., Hegedűs, E., Komminaho, K., Legostaeva, O., Tiira, T., Tolkunov, A., 2013. Seismic velocity model of the crust and upper mantle along profile PANCAKE across the Carpathians between the Pannonian Basin and the East European Craton. Tectonophysics 608, 1049–1072.

URL-Ihttp://en.climate-data.org/ (last visited on June 6th 2019).

URL-IIhttp://www-naweb.iaea.org/napc/ih/IHS_resources_gnip.html (last visited on June 6th 2019).

Velasco, V., Sanchez, C., Papoutsis, U., Antoniadi, S., Kontoes, C., Aifantopoulou, D., Paralykidis, S., 2017. Ground deformation mapping and monitoring of salt mines using InSAR technology. In: Proceedings of the Solution Mining Research Institute (SMRI) Fall 2017 Technical Conference. Münster, Germany. pp. 25–26 September 2017.